Proceedings of the 7th World Congress on Mechanical, Chemical, and Material Engineering (MCM'21)
~~Prague, Czech Republic~~ Virtual Conference – August, 2021
Paper No. ICCPE 105
DOI: 10.11159/iccpe21.105

Possible Effects of a Natural Silica-Based Sand on the Thermodynamic and Kinetic Behaviour of CH_4 and CO_2 Hydrate Formation.

Alberto Maria Gambelli[1*], Andrea Nicolini[1]
University of Perugia, Engineering Department
Via G. Duranti 93, 06125, Perugia, Italy
albertomaria.gambelli@unipg.it; andrea.nicolini@unipg.it

Abstract **-** Natural gas hydrate is one of the most promising energy source present worldwide; however, before make its exploitation feasible for large-scale applications, several improvements, in terms of process efficiency, are required. In this article, a specific silica-based natural sand, coming from the Mediterranean seafloor, was used as host for hydrate structures, produced in laboratory both in presence of methane or carbon dioxide. For experiments were carried out and thermodynamic and kinetic parameters were continuously monitored during hydrate formation. Then results were discussed and compared with ideal values for hydrate formation, easily found in literature. That specific sand was found to act as inhibitor for hydrate formation, in presence of both types of guests: the experimental formation curve remained constantly above the ideal one. However, several differences were found to exist between methane and carbon dioxide hydrate formation, in terms of moles of hydrate formed, saturation degree of sand pores, gas uptake, time required to complete the process and so on. Those latter differences are extremely important because they could be decisive in establishing how intervene in a specific hydrate reservoir.

Keywords**:** Natural gas hydrate; natural porous medium; chemical inhibitors; CO_2 storage.

1. Introduction

Hydrate of natural gas is a solid crystalline compound, where water molecules form solid cages and act as hosts, while gaseous molecules remain trapped inside those cages and thus act as guests [1]. In nature, natural gas hydrate (NGHs) is mainly diffused in marine sediments (≈97%) and in permafrost regions (≈3%) [2]. Considering that the dissociation of 1 m^3 of hydrate may release up to 164 m^3 of methane and only 0.8 m^3 of water, those natural reservoirs are gaining a growing interest as future energy source [3]. Based on the last estimations, the energy contained in hydrate reservoirs is over twice than the total energy producible from all conventional energy sources put together [4]. Moreover, NGHs have the advantage of being exploited as carbon neutral energy source [5]. In the last decades, different techniques have been performed to recover methane from those reservoirs; the most diffused are depressurization [6], thermal stimulation [7], chemical inhibitor injection [8, 9] or a combination of them.

The effectiveness of those application strongly depends by parameters like heat and mass transfer, porosity and permeability of the reservoir, its saturation degree, and so on. From here the need of a more deepened comprehension of the hydrate dissociation mechanism in function of elements commonly present in NGH reservoirs. Selim et al. [10] carried out a model to evaluate the heat and mass transfer during CH_4 hydrate dissociation in presence of a porous media; they found that the heat transfer mechanism mainly depends by the surrounding sediments. In addition, hydrate dissociation generates free water molecules, which immediately form an adherent layer on the surface of hydrate structures [11]. This latter aspect was also found in presence of a porous medium, where it led to a reduction of the hydrate dissociation rate [12].

Further consideration which must be made during NGHs exploitation are risks of soil deformations and failures, ice generation, excessive water production and sand production. In particular, ice generation strongly reduces the methane hydrate dissociation rate. Thus, the necessity of exploring new innovative solutions to intervene on hydrate reservoirs and the need to understand in advance if a specific reservoir is feasible for energy production, both under an economic and environmental point of view.

A new potential application consists in the water flow erosion. Such method is based on increasing the chemical potential of water and enlarging the difference in hydrate composition above the phase equilibrium, in order to hinder hydrate re-formation and ice production [13]. The water flow erosion method is also able to improve the heat and mass transfer and leads to an increase of salinity in the reservoir. Conversely, natural parameters as water composition, soil composition and morphology and so on, may intervene significantly. In previous works, it was been proved that the presence of sodium chloride represents a valid help in performing the CO_2/CH_4 exchange in hydrate reservoirs, with the double advantage of recovering methane to produce energy and storing carbon dioxide, making this energy source completely carbon neutral [14]. Rather than sodium chloride, further elements, commonly present in seawater, where found able to modify the classical trend of the hydrate formation and/or dissociation process [15].

In this article, methane hydrate and carbon dioxide hydrate formation were tested in presence of a silica-based sand, coming from the Mediterranean seafloor. Instead of the classical pure quartz sand, usually adopted in laboratory experiments, due to its weak influence on the process, which is exclusively limited to its physical properties, this natural sand shows the presence of several compounds, some of them already known to be chemical inhibitors for hydrate formation; moreover, it has a heterogeneous granulometry. Results were expressed in terms of moles of guest involved in the process and a particular attention was paid to the kinetic of the process.

2. Materials and methods

In this section, only materials involved and methods followed to carry out experiments have been carefully detailed. Information about the experimental apparatus is available elsewhere in literature [16 – 18].

2.1. Materials

The reactor was filled with 0.236 l of water and 0.744 l of sand. Considering sand grains characteristics and, in particular, its porosity, the free volume available for gas injection is equal to 0.22 liters. Pure carbon dioxide and methane were used, having a purity degree respectively equal to 99.99% and 99.97%.

The natural sand tested in this work was directly picked-up from the Mediterranean seafloor, near to the Tunisian costs. Table 1 describes the chemical composition of sand, while Figure 1 shows a diagram indicating its grainsize distribution.

Table 1. Chemical composition of sand.

Compound	Concentration [%]
SiO_2	99.1
Al_2O_3	0.25
Fe_2O_3	0.045
TiO_2	0.03
CaO	0.06
MgO	0.05
K_2O	0.11
Na_2O	0.05

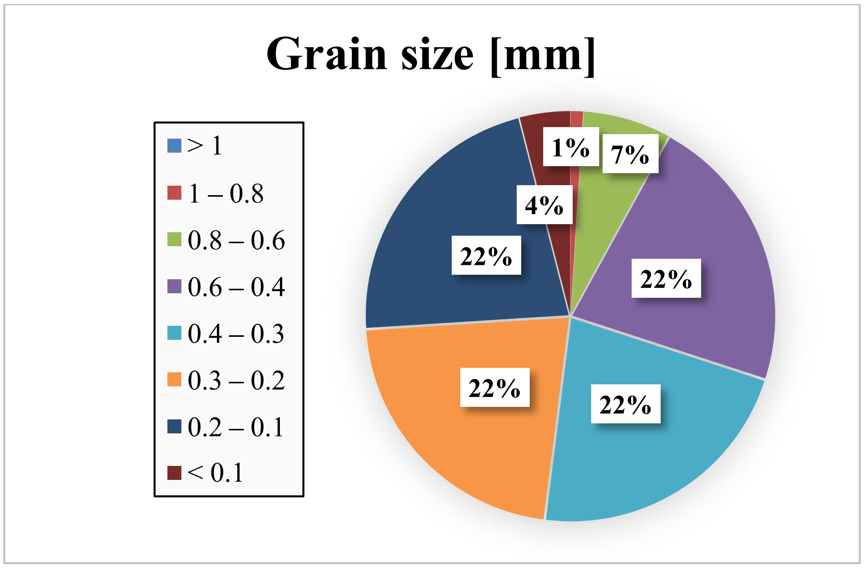

Figure 1. Grainsize distribution.

2.2. Methods

An initial gas stream was provided to completely remove air, if present. At the same time, temperature was brought to 1-3 °C. Then the ejection valve was closed and the gas was injected inside the reactor till reaching the desired pressure value. Once the injection phase finished, the reactor was closed in order to work in batch conditions. Thanks to the favourable thermodynamic conditions, hydrate formation immediately occurred with an initial increase in temperature, due to the exothermicity of the reaction, and a decrease in pressure, because of the entrapment of gaseous guest molecules. As soon pressure assumed a constant value, hydrate formation was considered finished. In each test, four specific points were selected and accurately described. The first point (PT1) represents the triggering of hydrate formation; the second (PT2) indicates the maximum temperature reached inside the reactor due to the reaction triggering. This latter point represents the finishing of hydrate nucleation and the beginning of the hydrate massive growth phase. Hydrate equilibrium is commonly described during its dissociation and not during formation, due to possible deviations from the ideal trend that usually occur during this latter phase. Such aspect was observed also in these tests and was described with PT3. Finally, PT4 described the ending of hydrate formation, and corresponds to the lowest pressure value measured during the experiment.

Parameters measured and calculated to describe those points have been argued in the following lines, while their values have been shown in the next section.

Letters “p” and “T” were used to indicate pressure and temperature, while time is represented with letter “t”. Moles of hydrate formed were indicated with “n_{HYD}”, and were calculated with Equation 1:

$$n_{HYD} = \frac{V_{PORE}(P_i Z_f - P_f Z_i)}{Z_f\left(RT - \frac{P_f}{\rho_{HYD}}\right)} \qquad (1)$$

In the equation: V_{PORE} is the free volume present inside sand pores, R is the gas constant, ρ_{HYD} is the ideal molar density of hydrate, calculated assuming 100% cage occupancy, and Z is the compressibility factor, calculated with the Peng-Robinson Equation.

The sand pores saturation degree, or SH, was calculated according to Equation 2:

$$SH = \frac{n_{HYD} * \frac{1}{\rho_{HYD}}}{V_{PORE}} \qquad (2)$$

Parameter H2OinHYD indicates moles of water involved in hydrate formation; it was calculated assuming a hydration number equal to 6, which corresponds to the formation of sI hydrate. H2Oliq represents moles of liquid water inside the reactor, while CH4g is the gaseous methane available for hydrate formation. Parameter [CH4g] is the percentage of gaseous methane in function of the H2Oliq and is expressed in molCH4gas/molH2Oliq.

GU% represents the gas uptake and was evaluated with Equation 3:

$$GU\% = \frac{CH_{4inj} - CH4_{g}}{CH_{4inj}} * 100 \qquad (3)$$

Where CH_{4inj} coincides with CH_{4g} at PT1.

According to what present in literature, hydrate formation was considered by assuming the first order reaction kinetic and hydrate formation was thus calculated with the following equations:

$$k = -\frac{1}{t} * \ln\left(\frac{CH_{4g}}{CH_{4g0}}\right) \qquad (4)$$

$$\frac{d_{CH4g}}{dt} = CH_{4g0} k e^{-kt} \qquad (5)$$

Finally, in all equations, subscripts "I" and "0" represent value measured for PT1, if the absolute value of the parameter was searched, or values related to the previous point, if the relative value was considered. In this latter case, subscript "rel" was used.

3. Results and Discussion

Four hydrate formation tests were carried out: half of them were made in presence of methane, while the others with carbon dioxide. For each test, a table showing all parameters of interest and a diagram, in which the pressure-temperature diagram is described, were provided. In particular, tables 2 and 3 and figures 2 and 3 represent respectively Test 1 and Test 2, carried out with methane, while tables 4 and 5 and diagrams 4 and 5 describe Test 3 and Test 4, made with carbon dioxide.

Table 2. Main parameters describing Test 1, carried out with methane.

	Test 1					
	PT1	PT2	PT3		PT4	
Parameters	Abs.	Abs.	Abs.	Rel.	Abs.	Rel.
P [bar]	66.53	64.45	61.35	--	45.47	--
T [°C]	2.93	4.39	-0.07	--	1.33	--
n_{HYD} [mol]	0	0.05	0.099	0.051	0.363	0.283
SH [%]	0	2.67	5.35	2.77	19.53	15.23
H_2O_{inHYD} [mol]	0	0.298	0.596	--	2.176	--
H_2O_{liq} [mol]	7	6.702	6.404	--	4.824	--
CH_{4g} [mol]	0.804	0.755	0.705	--	0.442	--
[CH_{4g}] [%]	11.49	11.26	11.01	--	9.15	--
GU% [%]	0	6.17	12.36	--	45.09	--
t [min]	0	116.25	667.92	551.67	11119.58	10451.67
k [1/min]	--	$5.47*10^{-4}$	$1.97*10^{-4}$	$1.24*10^{-4}$	$5.39*10^{-5}$	$4.47*10^{-5}$
dCH_4/dt [mol/min]	--	$-4.1*10^{-4}$	$-1.4*10^{-4}$	$-8.7*10^{-5}$	$-2.4*10^{-5}$	$-1.97*10^{-5}$

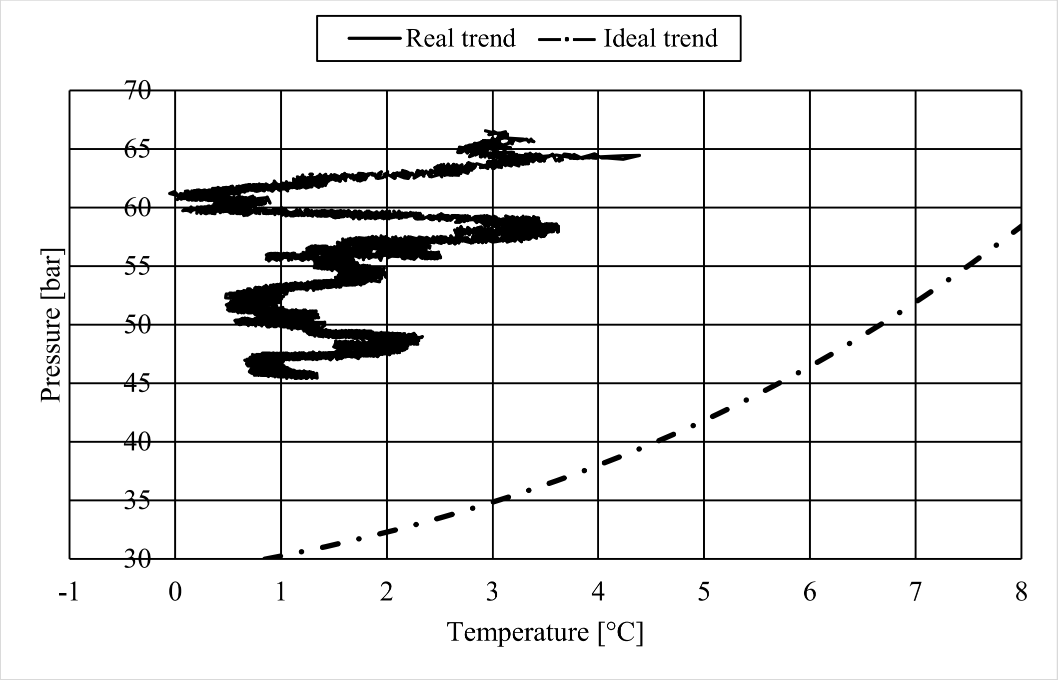

Figure 2. Pressure vs. temperature in Test 1 and comparison with the ideal trend.

Table 3. Main parameters describing Test 2, carried out with methane.

	Test 2					
	PT1	PT2	PT3		PT4	
Parameters	Abs.	Abs.	Abs.	Rel.	Abs.	Rel.
P [bar]	66.63	64.7	62.93	--	45.66	--
T [°C]	2.1	4.71	-0.17	--	0.84	--
n_{HYD} [mol]	0	0.05	0.072	0.022	0.364	0.308
SH [%]	0	2.71	3.87	1.21	19.62	16.57
H_2O_{inHYD} [mol]	0	0.302	0.432	--	2.185	--
H_2O_{liq} [mol]	7	6.699	6.569	--	4.815	--
CH_{4g} [mol]	0.81	0.76	0.738	--	0.446	--
[CH_{4g}] [%]	11.57	11.34	11.24	--	9.26	--
GU% [%]	0	6.21	8.88	--	44.96	--
t [min]	0	72.08	268.75	196.67	9978.33	9709.58
k [1/min]	--	$8.89*10^{-4}$	$3.46*10^{-4}$	$1.47*10^{-4}$	$5.98*10^{-5}$	$5.19*10^{-5}$
dCH_4/dt [mol/min]	--	$-6.8*10^{-4}$	$-2.6*10^{-4}$	$-1.1*10^{-4}$	$-2.7*10^{-5}$	$-2.31*10^{-5}$

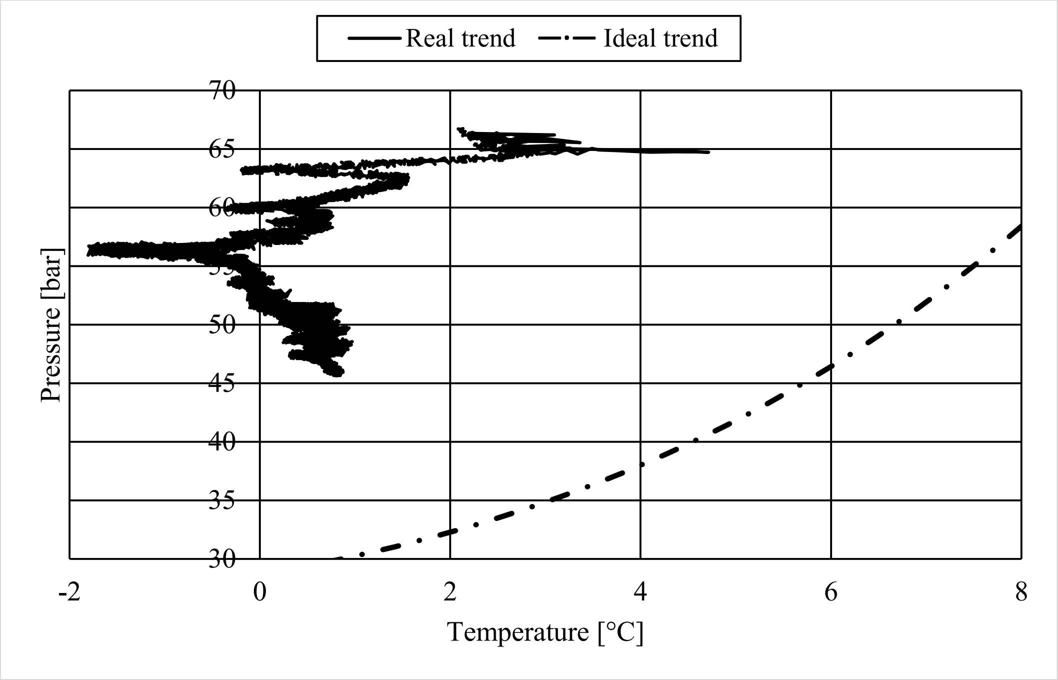

Figure 3. Pressure vs. temperature in Test 2 and comparison with the ideal trend.

Table 4. Main parameters describing Test 3, carried out with carbon dioxide.

	Test 3					
	PT1	PT2	PT3		PT4	
Parameters	Abs.	Abs.	Abs.	Rel.	Abs.	Rel.
P [bar]	40.37	--	--	--	30.27	--
T [°C]	9.15	--	--	--	0.42	--
n_{HYD} [mol]	0	--	--	--	0.141	--
SH [%]	0	--	--	--	7.58	--
H_2O_{inHYD} [mol]	0	--	--	--	0.844	--
H_2O_{liq} [mol]	7	--	--	--	6.156	--
CH_{4g} [mol]	0.433	--	--	--	0.293	--
[CH_{4g}] [%]	6.19	--	--	--	4.75	--
GU% [%]	0	--	--	--	32.47	--
t [min]	0	--	--	--	1407.92	--
k [1/min]	--	--	--	--	$2.79*10^{-4}$	--
dCH_4/dt [mol/min]	--	--	--	--	$-8.2*10^{-5}$	--

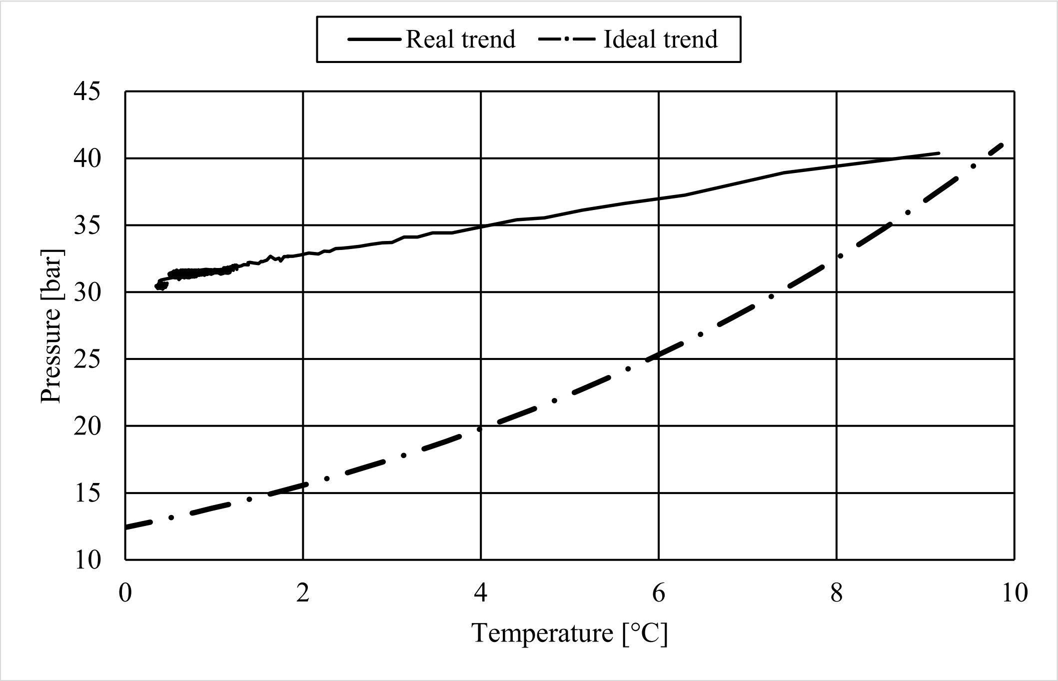

Figure 4. Pressure vs. temperature in Test 3 and comparison with the ideal trend.

Table 5. Main parameters describing Test 4, carried out with carbon dioxide.

	Test 1					
	PT1	PT2	PT3		PT4	
Parameters	Abs.	Abs.	Abs.	Rel.	Abs.	Rel.
P [bar]	40.59	37.48	--	--	31.13	--
T [°C]	4.3	9.27	--	--	0.38	--
n_{HYD} [mol]	0	0.053	--	--	0.138	0.088
SH [%]	0	2.84	--	--	7.44	4.71
H_2O_{inHYD} [mol]	0	0.316	--	--	0.829	--
H_2O_{liq} [mol]	7	6.684	--	--	6.171	--
CH_{4g} [mol]	0.447	0.394	--	--	0.309	--
[CH_{4g}] [%]	6.38	5.9	--	--	5.0	--
GU% [%]	0	11.81	--	--	30.94	--
t [min]	0	1.25	--	--	1403.33	1402.08
k [1/min]	--	0.1005	--	--	$2.64*10^{-4}$	$1.74*10^{-4}$
dCH_4/dt [mol/min]	--	-0.03961	--	--	$-8.1*10^{-5}$	$-5.4*10^{-5}$

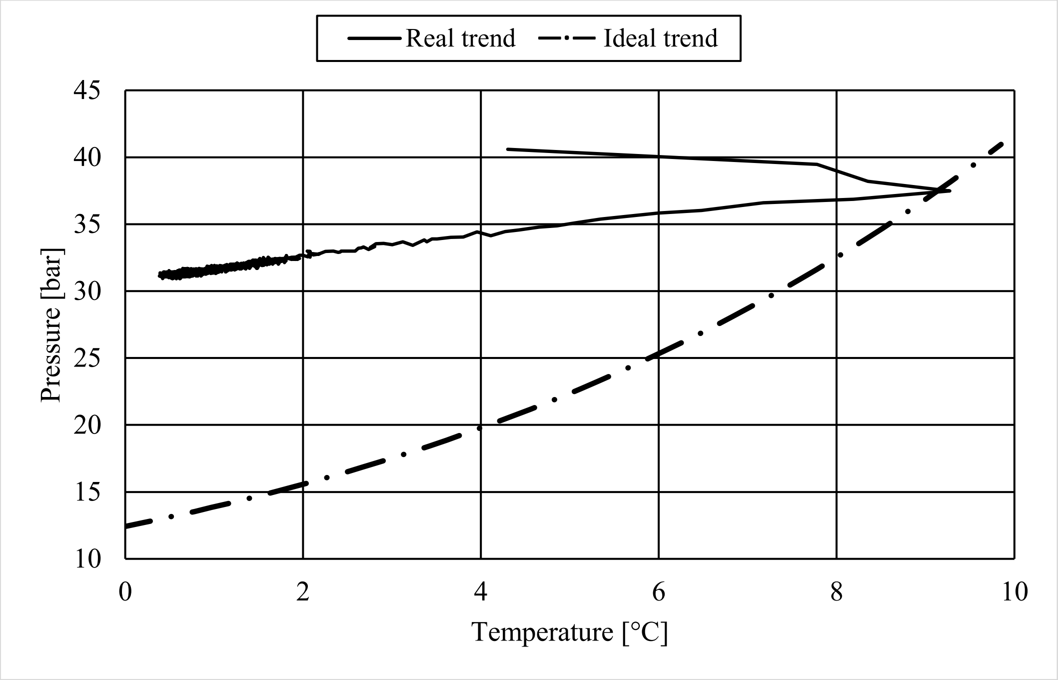

Figure 5. Pressure vs. temperature in Test 4 and comparison with the ideal trend.

The main characteristic, well highlighted in all diagrams, is the tendency of the present sand to act as inhibitor for the hydrate formation process. During all experiments, the real trend remained significantly above the ideal one, which has been drawn with a dashed line. That behaviour was noticed in presence of both types of guest; however, it was more pronounced in presence of methane, where P-T values, measured during hydrate formation, remained extremely far from the ideal equilibrium curve from the beginning to the ending of the test. Conversely, CO_2 hydrate formation started at thermodynamic conditions close to the ideal values, for then taking distance. In Test 4, the temperature peak due to the reaction triggering, generated an overlap between the two curves: for that reason, in the present test PT2 is slightly at right of the equilibrium curve. As explained before, the inhibiting influence exercised by this natural sand, is mainly due to the presence of further elements, rather than SiO_2 and, in particular, several oxides containing sodium, magnesium and also heavy metals, iron and so on.

In addition, some important differences, between tests made with methane and tests made with carbon dioxide, were noticed and need to be argued. Obviously, the initial pressure is lower in presence of CO_2, due to the ability of such compound to form hydrate at milder thermodynamic conditions than methane. For that reason, Test 1 and 2 started at 66-67 bar, while Test 3 and 4 at 46-47 bar. About moles of hydrate formed, better results were reached in presence of methane, where 0.363 – 0.364 mol of CH_4 were encaged into hydrate. However, this latter parameter does not represent a valid criterion to compare the two types of test, due to the difference in the initial quantity of gas injected inside the reactor. In addition, in tests made with CO_2, a further contribution, in terms of gas storage, must be mentioned. While the solubility of methane in water in negligible, a considerable amount of gaseous CO_2 dissolved in water. It was already proved in literature that in such case, considering the current thermodynamic conditions, dissolved CO_2 molecules will be surely involved in hydrate formation, even if the process will be slower [19]. More useful parameters are the saturation degree (SH) and the gas uptake (GU%). About the first, better results were obtained in presence of methane, where the final saturation, measured in PT4, ranged from 19.53 to 19.62. In the other case, SH was equal to 7.44 – 7.58, or extremely lower than the previous. Less different results were reached with GU%: 44.96 – 45.09 in Tests 1 and 2, and 30.94 – 32.47 in Test 3 and 4. Even if those values confirm a higher tendency of methane (than CO_2) of being involved in hydrate formation, a little opposite behaviour was noticed in terms of hydrate formation rate: time required to store CO_2 was enormously lower than that for methane. In the first two tests, 9710 – 10452 minutes were needed, while in the others only 1403 – 1408 minutes. It means that, in the same time lapse, a greater quantity of carbon dioxide can be stored on form of hydrate, if compared with methane.

A further relevant difference was noticed in the overall trend of each test. In presence of methane, the four points described in the previous section are well visible. Once feasible conditions for hydrate formation were established inside the reactor (PT1), the reaction occurred, with a visible temperature peak (PT2). Even if all real points differed from the ideal values, it is possible to see a specific area in which the two trends showed the most relevant difference among each other (PT3). Conversely, in tests carried out with carbon dioxide, the definition of each specific point was more difficult and not always possible. In both cases, PT3 and PT4 coincided. From diagrams it clearly appears that CO_2 hydrate formation occurred with a more linear trend, where a clear deviation from the ideal curve was defined, which remained constant over time. For that reason, the greatest difference between real and ideal trend was measured in correspondence of the process ending. In a similar manner, also PT1 and PT2 coincided, proving that the temperature peak, due to the reaction triggering, started immediately, without any delay compared to the gas injection phase. That description is feasible also for Test 4: in its diagram, the presence of a temperature peak is well visible, however the time lapse between PT1 and PT2 is only 1.25 minutes. Considering the time duration of the whole process, it can be concluded that the two points coincided.

4. Conclusion

The present work deals with the study of a natural silica-based sand, coming from the Mediterranean seafloor and, in particular, the analysis of its effects on the hydrate formation process. Four tests were carried out, half of them by using methane as guest compound, while the others involved carbon dioxide. Both thermodynamic and kinetic aspects were taken into account. The goal of the present research consisted in proving and also characterizing the potential influence that a specific soil may exercise on the hydrate sediment in it contained. That influence may intervene significantly during a lot of possible applications, such as gas storage, gas recovery from reservoirs, replacement strategies, currently explored to perform carbon neutral energy production, and so on.

That specific sand was found to be a inhibitor for hydrate formation: in both cases, the real hydrate formation trend constantly remained above the ideal one. In tests carried out with methane as guest, better results were reached in terms of gas uptake and moles of hydrate formed; however, considering the time lapse necessary to complete the process, a higher hydrate formation rate was noticed in tests carried out with carbon dioxide. Finally, in CO_2-based tests, a more coherent trend was observed, due to the less time required and to the greater ease of being trapped of carbon dioxide.

Future works will be focused on characterisation of other porous media coming from the Mediterranean Sea, due to the growing interest of research institutes and industries on hydrate reservoirs, which have been simulated or directly discovered, in this basin.

References

[1] A.M. Gambelli, F. Rossi. Natural gas hydrates: Comparison between two different applications of thermal stimulation for performing CO_2 replacement strategies. Energy, 172 (2019) 423 – 434.

[2] X.Y. Li, X.S. Li, Y. Wang, J.W. Liu, H.Q. Hu. The optimization mechanism for gas hydrate dissociation by depressurization in the sediment with different water saturations and different particle sizes. Energy, 215 (2021) 119129.

[3] J. He, X. Li, Z. Chen, Q. Li, Y. Zhang, Y. Wang, Z. Xia, C. You. Combined styles of depressurization and electrical heating for methane hydrate production. Applied Energy, 282 (2021) 116112.

[4] A.M. Gambelli, B. Castellani, A. Nicolini, F. Rossi. Water Salinity as Potential Aid for Improving the Carbon Dioxide Replacement Process' Effectiveness in Natural Gas Hydrate Reservoir. Processes, 8 (2020) 1298.

[5] A.M. Gambelli. An experimental description of the double positive effect of CO_2 injection in methane hydrate deposits in terms of climate change mitigation. Chemical Engineering Science (2021), doi: https//doi.org/10.1016/j.ces.2020.116430.

[6] V.C. Nair, S.K. Prasad, R. Kuma, J.S. Sangwai. Energy recovery from simulated clayey gas hydrate reservoir using depressurization by constant rate gas release, thermal stimulation and their combinations. Applied Energy, 225 (2018) 755–68.

[7] Gambelli AM, Rossi F. Thermodynamic and kinetic characterization of methane hydrate nucleation, growth and dissociation processes, according to the Labile Cluster Theory. Chemical Engineering Journal (2021), doi: https://doi.org/10.1016/j.cej.2021.130706.

[8] A.M. Gambelli, M. Filipponi, A. Nicolini, F. Rossi. International Multidisciplinary GeoConference: SGEM; Sofia Vol. 19, Fasc. 4.1 : 333 – 343. Sofia: Surveying Geology & Mining Ecology Managment (SGEM). (2019) DOI: 10.5593/sgem2019/4.1/S17.043.

[9] A.M. Gambelli, F. Rossi. The use of sodium chloride as strategy for improving CO_2/CH_4 replacement in natural gas hydrates promoted with depressurization methods. Arabian Journal of Geosciences, 13 (2020) 898.

[10] M.S. Selim, E.D. Sloan. Heat and mass transfer during the dissociation of hydrates in porous media. AIChE Journal, 35(1989) 1049 – 1052.

[11] V.A. Kamath, G.D. Holder. Dissociation heat-transfer characteristics of methane hydrates. AIChE Journal, 33 (1987) 347 – 350.

[12] J.W. Ullerich, M.S. Selim, E.D. Sloan. Theory and measurement of hydrate dissociation. AIChE Journal, 33 (1987) 747 – 752.

[13] B.B. Chen, H.R. Sun, H. Zhou, M.J. Yang, D.Y. Wang. Effects of pressure and sea water flow on natural gas hydrate production characteristics in marine sediment. Applied Energy, 238 (2019) 274–83.

[14] A.M. Gambelli, B. Castellani, M. Filipponi, A. Nicolini, F. Rossi. Chemical inhibitors as potential allied for CO2 replacement in gas hydrates reservoirs: Sodium chloride case study. Proceedings of the World Congress on Mechanical, Chemical, and Material Engineering (2020) 1-8, ICCPE 111.

[15] U. Tinivella. A method to estimate gas hydrate and free gas concentrations in marine sediments. Bollettino di Geofisica Teorica ed Applicata. 1999; 40: 19-30.

[16] A.M. Gambelli, B. Castellani, M. Filipponi, A. Nicolini, F. Rossi. Experimental analysis on the CO_2/CH_4 Replacement Efficiency due to Sodium Chloride Presence in Natural Gas Hydrates Reservoirs. E3S Web of Conferences, 197 (2020) 08008.

[17] A.M. Gambelli, B. Castellani, A. Nicolini, F. Rossi. Gas hydrate formation as a strategy for CH4/CO2 separation: Experimental study on gaseous mixtures produced via Sabatier reaction. Journal of Natural Gas Science and Engineering, 71 (2019) 102985.

[18] F. Rossi, A.M. Gambelli, D.K. Sharma, B. Castellani, A. Nicolini, M.J. Castaldi. Experiments on methane hydrates formation in seabed deposits and gas recovery adopting carbon dioxide replacement strategies. Applied Thermal Engineering, 148 (2019) 371 – 381.

[19] A.M. Gambelli, U. Tinivella, R. Giovannetti, B, Castellani, M. Giustiniani, A. Rossi, M. Zannotti, F. Rossi. Observation of the Main Parameters Influencing the Formation of Gas Hydrates. Energies, 14 (2021) 1803, https://doi.org/10.3390/en14071803.